Thermally and Vibrationally Induced Tautomerization of Single Porphycene Molecules on a Cu(110) Surface

Takashi Kumagai,[1] Felix Hanke,[2,†] Sylwester Gawinkowski,[3] John Sharp,[2] Konstantinos Kotsis,[2] Jacek Waluk,[3] Mats Persson,[2,4] and Leonhard Grill[1,5,*]

[1]*Department of Physical Chemistry, Fritz-Haber Institute of the Max-Planck Society, Faradayweg 4-6, 14195 Berlin, Germany*
[2]*Surface Science Research Centre and Department of Chemistry, University of Liverpool, Liverpool L69 3BX, United Kingdom*
[3]*Institute of Physical Chemistry, Polish Academy of Sciences, Kasprzaka 44/52, 01-224 Warsaw, Poland*
[4]*Department of Applied Physics, Chalmers University of Technology, 41296 Göteborg, Sweden*
[5]*Department of Physical Chemistry, University of Graz, Heinrichstrasse 28, 8010 Graz, Austria*
(Received 3 September 2013; published 11 December 2013)

We report the direct observation of intramolecular hydrogen atom transfer reactions (tautomerization) within a single porphycene molecule on a Cu(110) surface by scanning tunneling microscopy. It is found that the tautomerization can be induced via inelastic electron tunneling at 5 K. By measuring the bias-dependent tautomerization rate of isotope-substituted molecules, we can assign the scanning tunneling microscopy-induced tautomerization to the excitation of specific molecular vibrations. Furthermore, these vibrations appear as characteristic features in the dI/dV spectra measured over individual molecules. The vibrational modes that are associated with the tautomerization are identified by density functional theory calculations. At higher temperatures above ~75 K, tautomerization is induced thermally and an activation barrier of about 168 meV is determined from an Arrhenius plot.

DOI: 10.1103/PhysRevLett.111.246101 PACS numbers: 68.37.Ef, 68.43.Fg, 71.15.Mb, 82.37.Gk

Hydrogen atom transfer reactions are among the most common elementary processes in chemistry and biology [1]. Intramolecular hydrogen atom transfer (i.e., tautomerization) is of particular interest as it is related to photochromism [2] and enzymatic reactions [3]. Although tautomerization has been investigated by vibrational and fluorescence spectroscopy in ensembles of molecules, only very few studies exist at the single-molecule level. Recently, tautomerization has been imaged in free-based naphthalocyanine [4], phthalocyanine [5], and porphyrin [6] molecules on surfaces by scanning tunneling microscopy (STM) where it was triggered by injecting tunneling electrons into the molecule, but the excitation mechanism remained unclear.

Here we report tautomerization of single porphycene molecules on a Cu(110) surface induced via the excitation of specific molecular vibrations or via thermal activation. Porphycene [Fig. 1(a)], a constitutional isomer of porphine (i.e., free-base porphyrin) [7], is a planar and aromatic molecule. However, in contrast to the square shape of porphine, porphycene has a rectangular geometry in its inner cavity. This shape results in a more linear arrangement of N-H$\cdots$N (with an angle of 152°) [8] and a rather small N-N distance of 2.63 Å [7] (as compared to 2.89 Å of porphine [9]) along one direction. As a consequence of this geometry a stronger intramolecular H bond (N-H$\cdots$N) is formed in the cavity of porphycene, which causes very different properties in the tautomerization. In the case of porphine, the *trans-trans* transition can be observed only at elevated temperatures (with a rate of 2×10^4 s^{-1} at 298 K [10]) while tautomerization of porphycene is extremely rapid even at room temperature (5.8×10^{11} s^{-1}) [11]. The remarkable contrast in these properties stems from a significant reduction of the barrier height and length for the tautomerization coordinate, due to the strong H bond mentioned above.

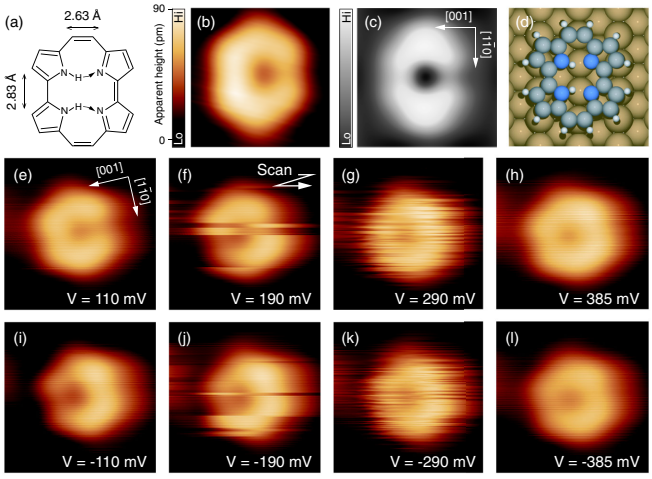

FIG. 1 (color online). (a) Molecular structure of porphycene (the hydrogen atom transfer during the *cis-cis* tautomerization is shown by arrows). The distances between the N atoms in the cavity [7] are indicated. (b) Typical STM image of a single porphycene molecule on Cu(110) (1.49×1.42 nm^2 in size; $I_t = 10$ nA and $V = 100$ mV). (c) The simulated STM image of the *cis*-1 configuration with the optimized structure in (d). (e)–(l) Voltage dependence of the STM image of a single porphycene molecule at 5 K. The bias voltage is indicated in each image and the tunneling current is set at $I_t = 5$ nA. The scan area is 2×2 nm^2 with a scanning time of about 9 sec /image.

Furthermore, it was found that the tautomerization properties in porphycene can be modified by introducing functional groups at the peripheral of the macroring [12,13]. Porphycene can also be considered a molecular switch that is reversibly transferred between two states [4,6,14–16]. Tautomerization is here of particular interest since switching does not involve any strong conformational change and might thus be compatible with incorporation of individual molecules into a nanoscale circuit.

STM is very suitable to study functional molecules on surfaces as it provides submolecular resolution and also allows the testing of the molecular function via the controlled manipulation of single molecules by various stimuli [17–21]. We performed our experiments in an ultrahigh vacuum chamber (base pressure of about 10^{-10} mbar), equipped with a low temperature STM (modified Omicron instrument with Nanonis Electronics). STM measurements were conducted at 5 K (if not specified differently) in constant-current mode (bias voltages refer to the tip voltage with respect to the sample). The Cu(110) surface was cleaned by repeated cycles of argon ion sputtering and annealing. Porphycene molecules were deposited [Fig. 1(a)] from a Knudsen cell (at a temperature of about 450 K). We obtained conductance spectra (dI/dV) with a lock-in amplifier with a voltage modulation of 12 mV at 710 Hz frequency.

Periodic density functional theory calculations were carried out using the Vienna *ab initio* simulation program (VASP) [22]. The electron-ion core interactions and the exchange-correlation effects were treated using the Projector Augmented Wave (PAW) method [23] and the optB86B version of the van der Waals density functional [24]. The Cu(110) surface was represented by a four layer slab with a 7×8 surface unit cell and a 17.63 Å vacuum region [25].

Figure 1(b) shows a typical STM image of a single porphycene molecule on Cu(110) that is characterized by a crescent-shaped protrusion with the long axis in the $[1\bar{1}0]$ direction of the surface, i.e., along the close-packed atomic rows of the surface. This asymmetric appearance represents the *cis* configuration (more precisely the *cis-1* configuration in contrast to the absent *cis-2* tautomer where the hydrogen atoms are located along the short side of the molecular cavity [26]) as becomes evident from a comparison with calculations [Figs. 1(c) and 1(d)]. Although the *trans* configuration is predicted to be the most stable in the gas phase [27] and by 77 meV in the present calculation over the *cis-1* configuration, we find that the latter is energetically favored on Cu(110) by 170 meV, due to the interaction of the nonhydrogenated N atoms with the copper row underneath. The *cis-2* configuration is energetically disfavored by about 1.3 eV in the gas phase and by about 1.1 eV for the adsorbed molecule. This theoretical result is in very good agreement with the experiment as no *trans* tautomer was ever found.

The STM image is static at low bias voltages at 5 K [as in Fig. 1(b)], but becomes fuzzy at higher bias voltages [Figs. 1(f) and 1(j)]. It can be clearly seen that at these voltages the molecule changes between two states which are determined as two (mirror-symmetric) *cis-1* (in the following named *cis* states) tautomer states from a comparison with static images [Figs. 1(e) and 1(i)]. This effect is also observed at step edges and in molecular assemblies, ruling out a rotation of the molecules that has a much higher energy barrier (at least 1.08 eV in our calculations). Hence, it reflects a *cis-cis* tautomerization in which the inner H atoms are transferred in the cavity [depicted in Fig. 1(a)]. Note that the molecule is located left or right by 0.02 nm of the close-packed copper row in the two tautomers and, consequently, slightly moves during tautomerization. This offset maximizes the interaction of the nitrogen atoms (without bonded hydrogen atoms) with the copper row underneath [as visible in Fig. 1(d)] [26].

The switching rate is enhanced when raising the bias voltage [Figs. 1(g) and 1(k)] as the tautomerization yield increases (discussed in detail below). Consequently, the switching between the two states cannot be resolved at high biases (due to the limited scanning speed of the STM) and the image appearance becomes symmetric [Figs. 1(h) and 1(l)] as the fluctuations are averaged out. Note that there is no difference in the appearance and behavior at positive and negative bias polarities.

At 5 K the porphycene molecules do not change their appearance in the STM images at low bias voltage (Fig. 1) and hydrogen atom transfer is never observed. However, at higher temperatures the transfer occurs spontaneously even at low bias voltages as can be seen in the insets of Fig. 2(a) where a bias voltage of 50 mV is used for imaging at 78 and 86 K. The fluctuations are equivalent to those in Figs. 1(e)–1(l), resulting from the tautomerization between the two *cis* states. It can be clearly seen that the switching rate increases with temperature (86 K as compared with 78 K), pointing to a thermally induced effect. To prove whether the process is merely induced by thermal activation or not, we investigated the current dependence of the tautomerization rate at 78 K [Fig. 2(a)]. Importantly, the

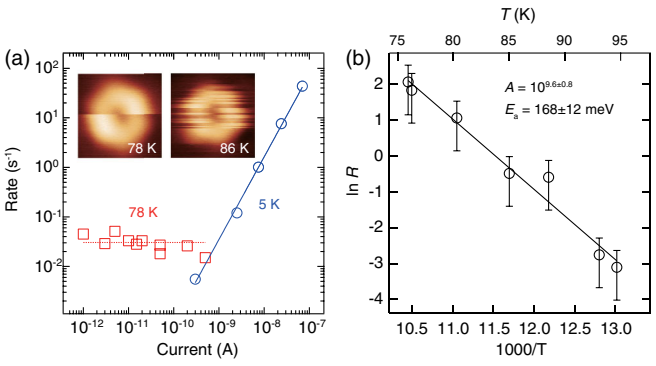

FIG. 2 (color online). (a) Current dependence of the tautomerization rate at different temperatures and bias voltages: 78 K and 50 mV (red squares) and 5 K and 200 mV (blue circles). The insets show STM images of a single molecule at 78 and 86 K. (b) Arrhenius plot of the thermally activated tautomerization (see text).

observed rate of about 0.03 Hz with a bias voltage of 50 mV (red squares) does not exhibit any dependence on the tunneling current, indicating that at 78 K the tautomerization is neither induced by the tunneling electrons nor the electric field in the STM junction and thus only a thermal process is involved. In contrast, the rate measured at 5 K with a bias voltage of 200 mV [shown for comparison in Fig. 2(a)] does depend on the tunneling current (as discussed in detail below). In addition, we measured the temperature dependence of the tautomerization rate, i.e., the Arrhenius plot [Fig. 2(b)], and find that the tautomerization rate R increases exponentially with the temperature which is characteristic for a thermally activated process [28,29]. The activation barrier E_a is determined as 168 ± 12 meV with the prefactor A of $10^{9.6\pm0.8}$ s^{-1} by fitting the data points with the Arrhenius equation [$R = A \times \exp(-E_a/kT)$].

STM-induced tautomerization can be observed in real time by recording the tunneling current over a molecule [Fig. 3(a)] while fixing the STM tip approximately over the inner H atoms in the molecular cavity. Hydrogen atom transfer induced by STM gives rise to a random-telegraph noise between the two states (i.e., high and low conductance), where each current jump corresponds to an individual switching event [Fig. 3(b) shows the schematics of the process]. Note that no other state than these two can be observed in the current trace, suggesting that either the process is fully concerted (i.e., the two hydrogen atoms are transferred simultaneously) or an intermediate *trans* configuration is not sufficiently stable to be detected within the STM time resolution (of about 1 ms).

The observation that the STM-induced tautomerization shows a clear threshold voltage and is equivalently induced at both bias polarities (Fig. 1) points to a tunneling electron mechanism rather than an electric field-induced effect, which is typically characterized by a polarity-dependent rate [30]. To further investigate the mechanism, we measured the current I dependence of the tautomerization rate R at various bias voltages [Fig. 3(c)] and find that the rate follows the power law of $R \propto I^N$. This behavior is very characteristic for inelastic electron tunneling processes [31], where N is related to the number of involved electrons.

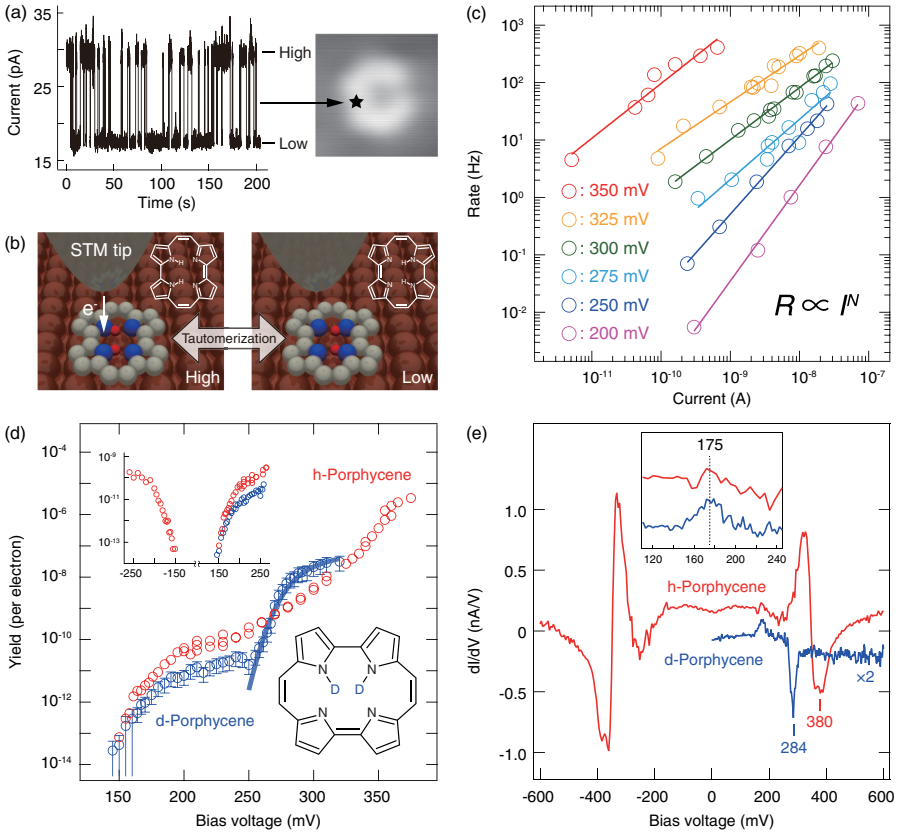

FIG. 3 (color online). (a) A typical current trace during a voltage pulse of 300 mV while the STM tip is fixed over a molecule (indicated by the black star in the image) with gap conditions of 100 mV and 10 pA. (b) Schematics of the tautomerization process. (c) Current dependence of the tautomerization rate at various bias voltages. The slopes (N) were determined as 1.67–0.05, 1.35–0.03, 1.05–0.11, 0.91–0.02, 0.81–0.04 and 0.95–0.09 for 200, 250, 275, 300, 325, and 350 mV, respectively. (d) Voltage dependence of the tautomerization yield for h- (red circles) and d-porphycene (blue circles) at 5 K (the latter is sketched in the inset). Yields above 380 mV cannot be determined due to our STM time-resolution of about 1 ms. A magnification of both bias polarities is shown on top. (e) dI/dV conductance spectra of single h- and d-porphycene molecules (after subtracting the background measured over the clean surface). The spectra were obtained at the same position as (a) with set points of 100 mV and 20 nA and 30 nA for h- and d-porphycene, respectively.

N is found to be about 1 for bias voltages above 275 mV, indicating a one-electron process, while it increases to 1.35 and 1.67 at bias voltages of 250 and 200 mV, respectively. This result might be interpreted as the crossover from one- to two-electron processes because of insufficient energy transfer to the tautomerization coordinate at lower bias voltages.

To gain a more detailed physical insight into the tautomerization mechanism, we also prepared an isotope-substituted molecule in which the hydrogen atoms in the cavity are replaced by deuterium [see inset of Fig. 3(d)]. When measuring the yield for hydrogen- and deuterium-substituted molecules (denoted by h- and d-porphycene, respectively) as a function of the bias voltage [Fig. 3(d)], we find a substantially different behavior at higher voltages. For d-porphycene a clear step can be observed in the range from 250 to 300 mV. Such a voltage dependence of the reaction yield can be theoretically reproduced [32] and the curve is mainly determined by the vibrational energy and a broadening factor, which is primarily attributed to the statistical error of the experimental data and can be described by a Gaussian profile [33]. Following this fitting procedure for the curve of d-porphycene [solid curve in Fig. 3(d), we obtain a vibrational energy of 279 ± 5 meV, which agrees well with the calculated N-D stretching mode (see Fig. 4 below), and a broadening factor of 21 meV. Hence, the tautomerization process occurs via the excitation of the N-D stretching mode in the cavity. Because the theory assumes only single-electron processes, we did not apply it to the lower threshold region. On the other hand, a rather moderate increase of the yield is observed for h-porphycene, which ranges from 250 to 380 mV. As discussed below, this increase is associated with the N-H stretching excitation and this mode is significantly broadened due to the strong anharmonicity in the mode potential.

Furthermore, we find that the strong coupling of vibrational excitation with the tautomerization results in nonlinear characteristics in the conductance curve measured over a molecule. The dI/dV spectra for individual h- and d-porphycene molecules in Fig. 3(e) show at both bias polarities a characteristic peak and dip at 175 and 380 mV for h-porphycene and a dip at 284 mV for d-porphycene, respectively. The isotope ratio of the dip positions (of 1.34) is in line with the simple ratio of the N-H and N-D reduced mass ($\sqrt{\mu_{\mathrm{ND}}/\mu_{\mathrm{NH}}} \approx 1.33$). Therefore, the dip, as well as the increase of the yield in Fig. 3(d), can be assigned to the N-H(N-D) stretching mode, in agreement with previous dI/dV observations of electron-induced molecular motions coupled to vibrational excitations [31]. It should be noted that a peak or dip position can be slightly shifted by a few mV from the vibrational energy [34]. However, we find a significant redshift from the N-H(N-D) stretching mode energies of 417 meV in free NH_3 [35] and of 412 meV in free-based porphyrin [36], indicating a strong hydrogen-bonding interaction in the cavity of the porphycene molecule.

Additionally, the dip is much broader for h-porphycene than for d-porphycene (note that an identical experimental resolution was used for both measurements), which is mainly attributed to the vibrational broadening effect caused by the anharmonic nature of the H-bonded N-H stretching. A recent theoretical study showed that the N-H stretching mode couples anharmonically with other low frequency modes, giving rise to a broadening of the vibrational density of states [37]. The broadening is expected to be smaller for the N-D stretching as the anharmonicity is less pronounced for deuterium [37], in agreement with our observations [Fig. 3(e)]. Note that this also agrees with the rather moderate increase in the yield curve of h-porphycene (around 370 mV) in contrast to the more distinct step at 279 mV for the isotope-substituted case [Fig. 3(d)]. In addition, the splitting of the dip can be observed only for the N-H stretching [in particular for a negative bias in Fig. 3(e)]. Because this splitting is totally absent in the N-D stretching, we assign it to a Fermi resonance [38], which results in the further broadening of the dip for h-porphycene.

On the other hand, the low energy peak at 175 meV that correlates with the threshold in the voltage dependence of the yield [Fig. 3(d)] remains at the same energy upon isotope substitution, thus pointing to a vibrational band with a negligible influence from hydrogen (or deuterium) displacement in the molecular cavity. Note that the vibrational band at 175 meV also matches the measured thermal barrier height of 168 meV [Fig. 2(b)], suggesting that this vibrational band plays a role in the tautomerization in both cases.

To gain further insight into the role of vibrational excitations in the tautomerization, we calculated the vibrational density of states of the adsorbed molecule on a rigid substrate and their projection on the in-plane displacements of the inner H(D) atoms and the N atoms (Fig. 4). The N-H(N-D) stretch modes are found to be at 376 (279) meV, in very good agreement with the experiments (380 and 275 meV), confirming our assignment above.

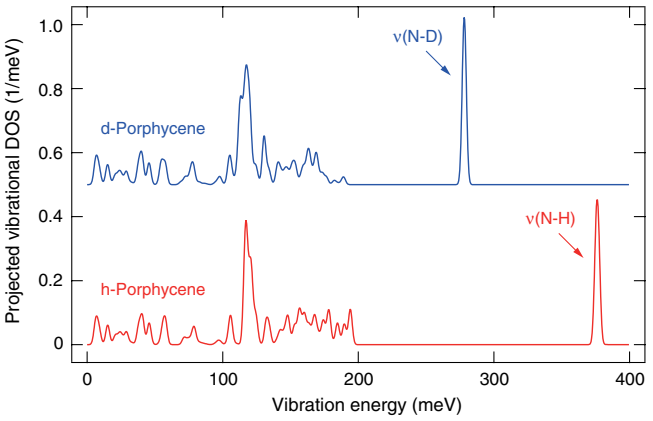

FIG. 4 (color online). Calculated projected vibrational density of states of the h-porphycene and the d-porphycene adsorbed on a rigid Cu(110) surface [the optimized structure is shown in the Fig. 1(d)]. The in-plane projection is on the displacements in the molecular plane of the two inner H atoms and the four N atoms. The discrete vibrational modes have been broadened by a Gaussian with a width of 2 meV [39].

Another band of in-plane modes, which correlate with the reaction coordinate of the tautomerization, is in the energy range from 120 to 180 meV. This energy range of vibrational modes matches with the onset (150 mV) of the STM-induced tautomerization and furthermore exhibits no apparent isotope effects (Fig. 4), both in agreement with our experiments. The observed peak at 175 meV cannot simply be attributed to a single vibrational mode but can have contributions from several modes involving in-plane vibrational motions of the N and H atoms that are strongly coupled with the out-of-phase motions of the C atoms and C-H bending motions. Furthermore, there are no out-of-plane modes in this energy range according to our calculations.

In conclusion, we have identified thermally and vibrationally induced tautomerization for single porphycene molecules on a Cu(110) surface. The first is characterized via the temperature dependence of the transfer rate. The vibrational excitation is determined by isotope substitution of the inner hydrogen atoms together with the bias voltage dependence of the tautomerization yield and identified as the N-H(N-D) stretching mode. Density functional theory calculations are in very good agreement with experimental results, both in the vibrational energies as well as the energetic shift caused by isotope substitution.

We thank the Japan Society for the Promotion of Science (T. K.), the German Science Foundation (SFB 658), the European Union (AtMol and ARTIST), the Polish National Science Centre (3550/B/H03/2011/40) and VR (M. P.) for financial support and EPSRC (EP/L000202) through MCC, SNIC, and PRACE for computer resources at HECTOR and PDC.

*Corresponding author.
leonhard.grill@uni-graz.at
†Present address: Accelrys, Ltd., 334 Science Park, CB4 0WN Cambridge, United Kingdom.

[1] J. T. Hynes *et al.*, *Hydrogen-Transfer Reactions* (Wiley-VCH, Weinheim, 2007).
[2] K. Tokumaru, T. Arai, and M. Moriyama, Mol. Cryst. Liq. Cryst. **246**, 147 (1994).
[3] O. Tapia, J. Andres, and V. S. Safont, J. Phys. Chem. **98**, 4821 (1994).
[4] P. Liljeroth, J. Repp, and G. Meyer, Science **317**, 1203 (2007).
[5] A. Sperl, J. Kröger, and R. Berndt, Angew. Chem., Int. Ed. **50**, 5294 (2011).
[6] W. Auwärter, K. Seufert, F. Bischoff, D. Ecija, S. Vijayaraghavan, S. Joshi, F. Klappenberger, N. Samudrala, and J. V. Barth, Nat. Nanotechnol. **7**, 41 (2012).
[7] E. Vogel, M. Köcher, H. Schmickler, and J. Lex, Angew. Chem., Int. Ed. Engl. **25**, 257 (1986).
[8] U. Langer, C. Hoelger, B. Wehrle, L. Latanowicz, E. Vogel, and H.-H. Limbach, J. Phys. Org. Chem. **13**, 23 (2000).
[9] L. E. Webb and E. B. Fleischer, J. Chem. Phys. **43**, 3100 (1965).
[10] J. Braun, M. Koecher, M. Schlabach, B. Wehrle, H.-H. Limbach, and E. Vogel, J. Am. Chem. Soc. **116**, 6593 (1994).
[11] P. Fita, N. Urbańska, C. Radzewicz, and J. Waluk, Chem. Eur. J. **15**, 4851 (2009).
[12] A. Vdovin, J. Waluk, B. Dick, and A. Slenczka, ChemPhysChem **10**, 761 (2009).
[13] M. Gil *et al.*, J. Am. Chem. Soc. **132**, 13 472 (2010).
[14] B. L. Feringa, *Molecular Switches* (Wiley-VCH, Weinheim, 2001).
[15] V. Iancu and S.-W. Hla, Proc. Natl. Acad. Sci. U.S.A. **103**, 13 718 (2006).
[16] C. Dri, M. V. Peters, J. Schwarz, S. Hecht, and L. Grill, Nat. Nanotechnol. **3**, 649 (2008).
[17] J. A. Stroscio and D. M. Eigler, Science **254**, 1319 (1991).
[18] W. Ho, J. Chem. Phys. **117**, 11 033 (2002).
[19] T. Komeda *et al.*, Science **295**, 2055 (2002).
[20] F. Moresco, Phys. Rep. **399**, 175 (2004).
[21] L. Grill, J. Phys. Condens. Matter **20**, 053001 (2008).
[22] G. Kresse and J. Furthmüller, Phys. Rev. B **54**, 11169 (1996).
[23] G. Kresse and D. Joubert, Phys. Rev. B **59**, 1758 (1999).
[24] J. Klimes, D. R. Bowler, and A. Michaelides, Phys. Rev. B **83**, 195131 (2011).
[25] The plane-wave cutoff was 400 eV. The atoms in the bottom two layers were constrained at their bulk positions during the relaxations with a calculated lattice constant of 3.60 Å. The structures were relaxed until all forces were less than 0.01 eV $Å^{-1}$. In the structural relaxations only the G point was kept in the k-point sampling while in the STM simulations a $2 \times 2 \times 1$ k-point grid was used.
[26] T. Kumagai *et al.*, Nat. Chem. (to be published).
[27] Y.-D. Wu, K. W. K. Chan, C.-P. Yip, E. Vogel, D. A. Plattner, and K. N. Houk, J. Org. Chem. **62**, 9240 (1997).
[28] T. Zambelli, J. Trost, J. Wintterlin, and G. Ertl, Phys. Rev. Lett. **76**, 795 (1996).
[29] M. Schunack, T. Linderoth, F. Rosei, E. Lægsgaard, I. Stensgaard, and F. Besenbacher, Phys. Rev. Lett. **88**, 156102 (2002).
[30] M. Alemani, M. V. Peters, S. Hecht, K.-H. Rieder, F. Moresco, and L. Grill, J. Am. Chem. Soc. **128**, 14 446 (2006).
[31] J. Gaudioso, L. J. Lauhon, and W. Ho, Phys. Rev. Lett. **85**, 1918 (2000).
[32] T. Kumagai, A. Shiotari, H. Okuyama, S. Hatta, T. Aruga, I. Hamada, T. Frederiksen, and H. Ueba, Nat. Mater. **11**, 167 (2012).
[33] K. Motobayashi, Y. Kim, H. Ueba, and M. Kawai, Phys. Rev. Lett. **105**, 076101 (2010).
[34] Y. Ootsuka, T. Frederiksen, H. Ueba, and M. Paulsson, Phys. Rev. B **84**, 193403 (2011).
[35] G. Herzberg, *Molecular Spectra and Molecular Structure II, Infrared and Raman Spectra of Polyatomic Molecules* (Van Nostrand, Princeton, 1945).
[36] J. G. Radziszewski, J. Waluk, and J. Michl, Chem. Phys. **136**, 165 (1989).
[37] S. Gawinkowski, Ł. Walewski, A. Vdovin, A. Slenczka, S. Rols, M. R. Johnson, B. Lesyng, and J. Waluk, Phys. Chem. Chem. Phys. **14**, 5489 (2012).
[38] T. Miyazawa, J. Mol. Spectrosc. **4**, 168 (1960).
[39] The spectrum of the adsorbed molecule on a rigid substrate lattice was calculated by diagonalizing the dynamical matrix that was obtained by finite differences of the calculated forces at symmetric ionic displacements of 0.01 Å.